Contract number : BREU-CT91-0519 (RZJE) ,

Project title : Precision Machining Spindles

Prime contractor : Nederlandse Philips Bedrijven BV

Names of the partners :

P	Philips	Nederlandse Philips Bedrijven BV
C	CP	Cranfield Precision Ltd
F	1 PT	Fraunhofer-Gesellschaft, Institut fur Produktionstechnologie
Z	Zeiss	Carl Zeiss Stifftung

Reference period : 01/11/1991 to 31/'10/1995

Report reference number : PMS-P-602-1

Table of Contents

ABSTRACT 3

Precision Machining Spindles 4
1. History before the project started 4
2. Introduction 5
3. preliminary study 5
3.1 High speed spindle specifications 5
3.2 Program rotor-bearing dynamics 6
3.3 Hybrid bearing calculation 6
3.4 Compare bearings, choose spindle 6
3.5 Design optimization tool 7
4. Prototype HSS design. 8
4.1 Design rotor and bearings. 8
4.2 Design machine mount 8
4.3 Design integrated cooling 8
5. prototype spindle analysis 9
5.1 Dynamic rotor/bearing analysis 9
5.2 StaticF E-analysis 10
5.3 Thermal analysis 10
6. Prototype manufacturing 11
6.1 Drawing 11
6.2 Manufacture, assembly and balancing 11
7. prototype high speed spindle tests 12
8. The second prototype 12
8.1 Prototype breakdown analysis 12
8.2 Design changes 13
9. Second prototype spindle measurements 14
9.1 Grinding experiments 1
9.1.1 Grinding experiments (CPE) 14
9.1.2 Grinding experiments (Zeiss) 15
9.1.3 Grinding experiments (Philips) 15
9.1.3 Analysis of grinding results 16
9.2 Thermal measurements (IPT) 16
9.3 Dynamic stiffness measurements (IPT) 16
9.4 Error motion measurements (CPE) 17
10. Final spindle redesign 18
10.1 Design changes 18
10.2 Analysis of the redesigned spindle 19
10.3 Manufacturing 19
11. Optimized design tests 2
11.1 Measure thermal behaviour 20
11.2 Grinding tests 20
11.3 Measure error motions 20
11.4 Measure dynamic behaviour 21
12. Conclusions 21

References 22

ABSTRACT

This report describes the, BRITE/EURAM project BE-519, Precision machining spindles. The main purpose of "our project was to develop a High Speed Spindle with properties beyond the ones of commercially, available spindles, to be able to produce better grinding results.hilips (Eindhoven). was the prime contractor and the-other partners were IPT Fraunhofer (Aachen), Cranfield precision and Carl Zeiss (Oberkochen) . For the, second half of the' project Hembrug was the End User (chapters 1 and 2) .

We started with an ambitious list of specifications beyond the ones of commercially available spindles. That illustrates that all partners were more end users than. spindle manufacturers. The project was guided by the strong believe that analysis (physical understanding plus calculation power) is needed to realise the '. spindle we were aiming at (chapter 3) .

Analysis and design were performed in parallel so both effected each other in good cooperation (chapters" 4 and 5) .

This report gives five cross sections of spindle designs at different stages in the project showing the evaluation into' a spindle that can be manufactured and used for actual high quality grinding.

The third design was actually manufactured as first prototype an already reached the 100,000 rpm (chapter 6' and 7) . That prototype crashed at 104,000 rpm after only three weeks of operation. After a breakdown analysis we found extra power losses neglected in the first analysis (chapter 8) . New calculations plus some design improvements were the basis for the second prototype that **was** manufactured. That second prototype' went on a tour' along all partners and was tested extensively during a one years perio chapter 9) .

Meanwhile the design work concentrated on manufacturing costs reduction and user friendliness. From 'that design four spindles were manufactured, one for each partner (chapter 10) .

Preliminary tests of this redesigned spindle are reported i chapter 11

Precision Machining Spindles

1. History before the project started

The need for a precision, machining spindle as developed in this project became evident'at Philips during measurements of grinding 'forces in February 1987. That work is part of a thesis from Dr J. Franse (reference 11). From his error budget (table I) it can be found that his. grinding spindle compliance" was the largest error source giving more than 70% of the total error.

Error source	Error [rim]	% of E_{tot}
x-slide motions ,	3.3	1.20
z-slide motions	3 . 8	1.38
Headstock run-out	20.,0	7 . 2 9
Reference mirror	0.5	0 . 1 8
Slide compliancies	0 . 5 '	0.18
Headstock compliance	0.4	, 0.15
Laser resolution	1 0 . 0	3 . 6 4
Thermal errors	30.0	10.9'3
Laser errors (refr. index)	6.	2.19
Grinding spindle compliance	2 0 0 . .	72.86 "'
Total' (worst case) error E_{tot}	274.5	100.

Table I. Form error budget of **ESDO** for a 5' mm ground mould

At November 04 1987 Philips Engineering department started to develop a high stiffness/high speed spindle according to their state of the art.
Philips and IPT started' cooperation on precision machining in March 1988, and in May 1988 they choose a high speed grinding ' spindle as carrier for that cooperation. When CPE and Zeiss also did show interest in this subject we started the preparation of a BRITE/EURAM proposal January 1989. That BRITE proposal dated August 17 1989 was rejected in January 1990. An adapted proposal (ref number 4445) went through a negotiation meeting in Brussels (February 13 1991). The work programme was adapted into version dated June 12 1991 and the proposal was granted to start November 01 1991 (in stead of July 01 1991) for a 3.5 years period.

A contract BREU-CT91-0519 (RZJE) was signed between:
The European Economic Community (Brussels Belgium)
a n d
Nederlandse Philips Bedrijven BV (Eindhoven The Netherlands)
Cranfield Precision Engineering **LTD** (Cranfield England)
Fraunhofer-Gesellschaft (Aachen Germany)
Carl Zeiss Stifftung (Oberko.then Germany)
with Hanseatische Praezision und Orbittechnik GmbH as End User

We asked for extension of the contract and the EEC agreed August 30 1994. So the duration of the project became 48 months from November" 1'1991 ending at 31 October 1995.
When HPO ceased. trading around mid term of' the project, Hembrug (Haarlem Holland) became our End User.

2. Introduction

The' main purpose of our project was to develop a High Spee Spindle (HSS) with properties beyond the ones o'f commercially available. spindles to be able to produce better grinding results The logical sequence of our project in work packages is first a *Preliminary study,* then the *HSS design,* thereafter the *HSS manufacturing* and *HSS tests* including grinding experiments. A simplified planning, of the whole project is given in figure 2.. After testing the prototype, another *cycle from design to* testing was planned to obtain optimized spindles.
The spindle specifications we aimed for were' that high that we could only reach them with narrow bearing gaps: As" a consequence, the manufacturing costs of a prototype HSS spindle were. far more than planned. That made us to concentrate on *manufacturing costs reduction* in the optimization stage.
The 'prototype spindle did run 100,000 rpm but eras'hed before we could perform -all measurements and grinding experiments. The breakdown analysis showed that the estimated spindle losses-wer far more than predicted and the reason for this was determined. As a consequence a second prototype, is manufactured based on nev calculations. That second prototype performed "well in the measurements. However that was at the .expense of half a year extension ". of the project duration. Finally four redesigned spindles were manufactured, one for each partner. Those spindles are" designed for actual use in production

3. Preliminary study

3.1 High speed spindle specifications

The high speed spindle specifications 'were . consolidated, see figure 3.1. The. most appealing *ones were:*

maximum rotating speed . . . . .1 . . . . . 100,000 rpm
radial stiffness at cutting edge . . . . 20 N/pm
axial 'stiffness at cutting edge . . . . . 20 N/pm ,
radial synchronous error motion . . . . . 50 nm
radial asynchronous error motion . . . . 20 nm
thermal drift ('after 10 minutes) .'. .. 10 nm

We did realize that some goals were rather ambitious, so we" included a list of HSS decision criterions illustrating the weight each partner gave to each subject.

3-.2 Program rotor-bearing dynamics

For the calculation of rotor-bearing dynamics we used the Philips ,. program RODY. The design is divided into elements like shafts, disks and the bearings are represented by springs and damper The element properties including gyroscopy are assembled and the "solution is found using PC-Matlab as a tool.

For compressible fluid bearings the original Philip's program **RODY** is extended in cooperation with Technical University of Eindhoven (references 2], **3]** and 4]) into RODY4 capable to handle compressible bearing coefficients (depending not only upon rotational speed but also upon excitation frequency) . .

3.3 Hybrid bearing calculation

We generated our own bearing coefficients because literature does not provide the numbers we need. At a very late state we decided that externally pressurized spiral groove bearings were favoured over orifice type bearings.

Starting from existing FEM programs, one, for calculating static behaviour of spiral groove bearings with compressible lubricants and one for calculating dynamic coefficients of externally pressurized bearings; Philips is, capable now to supply the data : needed for the dynamic RODY analysis.

For the thrust bearing we extended existing' computer code with dynamic elements" to calculate stiffness (and damping) o-f externally pressurized spiral groove compressible bearings. Unexpectedly we found that such thrust bearings become unstable above a certain critical speed. Higher supply pressures have a stabilizing effect.

The programs were also adapted to calculate partially tapered gaps to enable us to predict the bearing properties with axi bearing 'clearances variations.

3.4 Compare bearings, choose spindle configuration

At our kick-off meeting we made a choice of four different designs out **of** nine proposals for further evaluation. Out of that evaluation we choose the conventional design with an integrated motor drive located between the journal bearings and with a conical front bearing that combined. axial and radial support (see figure 3.2). We choose for an integrated motor in between the bearings because we have no better ideas than existing designs that cannot guarantee precision at high speeds.

The choice for spiral groove bearings over orifice bearings is made because of design considerations. (no separate radial supply channels to each restrictor needed) . One should realize that in journal bearings the spiral grooves make the bearing stable in concentric operation. Smooth journal bearings have a larger load carrying capacity but are not stable until the eccentricity is more than about half the gap height. The external pressurization is primarily intended for contactless starting up and stopping

(no wear) but also results in higher stiffness and better stability (because the 'air behaves more incompressible). Pressurization of spiral groove bearings also constitutes a spiral groove motor, in' our case the spindle runs at about 5,000 rpm without'motor drive and has enough power for diamond cutting of small pieces (we used that for machining a 20 mm diameter aluminum master).

3.5 Design optimization tool

The bearing configuration of a spindle must meet many different requirement,s as good as possible. To be able to make a rational choice between different types of bearings that at first sight look promising, an optimization had to be carried out first fo'r these types of bearings.

A constraint non-linear optimization,problem was formulated 'in 'the following manner:

A" 'basic geometry of the spindle bearing configuration was defined, for instance 2-bearing and 3-bearing designs. The diameters, lengths and the bearing gaps, can be chosen to obtain optimal radial stiffness at the cutting edge. The radial compliance at the 'cutting edge was taken as the criterion to be minimized under constraints like:

Total Friction losses in the radial bearings <= 250 Watt.
Bearing gaps >= 5 µm. ."
.Shaft" diameter <= 10 mm and shaft length >= 20 mm at motor location.
Total length of the rotor < "200 mm.

To carry out this optimization, software was' written in PC-Matlab. Basically, from a guessed starting situation, the program evaluates the stiffness and the temperature distribution in the system using finite element calculations and tests" whether all constraints are met. If one or more constraints are violated, the program uses a simplex method to search for adjustments of the geometrical parameters so as to come into the solution space, where all the constraints are met. Within the solution space., quadratic programming is than used to search for an optimal, situation..

Calculations were carried out u'sing 50.000 and 100.000 rpm as running , speeds. It was evident that the clearance constraint becomes the active constraint in nearly all cases, before' the power constraint.

That optimization tool showed that hydrostatic bearings were not a good bearing type to apply for a high speed spindle because. of heat generation and, power loss. Externally pressurized tapered . gap bearings without restrictors could not achieve high enough stiffness to meet our specifications. The final choice between, externally pressurized conical gap bearings with inlet restrictors and externally pressurized spiral groove bearings could not be made on the basis. of the optimization tool because their characteristics differed less than the accuracy of the method.

A very "important characteristic of the spindle is its dynamic behaviour. "The lowest natural frequency of the system "should

occur well above the running speed. **A** part of **RODY** (with consta springs for the bearings) was added to check the lowest natural frequency afterwards.

4. Prototype HSS design

4.1 Design rotor and bearings

Initially it was decided that the grinding spindle was to be a two bearing spindle with" 'an integrated electro motor fitted, between those bearings. The conical front bearing was abandoned early because of its 'manufacturing consequences. T-he optimization tool showed that bending of the shaft limited the overall spindle stiffness. Therefore a three bearing concept was worked out first with an extra bearing situated between the thrust bearing and t electro motor see figure 4.1.
The optimization tool showed that two types of bearings could be chosen conical gap bearings with orifices or spiral groove bearings. Both nee-d 12 bar-air supply" pressure to achieve the specified high stiffness. Conical gap-bearings are fairly eas to make. Spiral "grooves are much more-difficult to make but "relatively easy to pressurize using a central air supply groove so minimizing the critical distance from cooler to bearing. Such design considerations made us to 'choose for externally pressurized spiral groove bearings.
The spindle is driven by an integrated electro motor with the rotor fixed directly to the spindle shaft. At manufacture the rotor. (assembled to the shaft) could be ground using the middle and the front bearing as a reference. This implicated that the back part of the spindle housing should be. fixed 'to the middle part in'such a way that grinding of the rotor is possible.
We choose "Boegra bronze for the housing and hardened stainless steel for the shaft. These materials are relatively easy, t machine, and have" a good wear resistance in case of seizure.

4.2 Design machine mount

For mounting the spindle we decided to use **a** spindle mount as integral part of the spindle 'to prevent housing deformations by improper assembly. A machine mount as interface to the machine , can be designed "to ones specific needs.
The front of the spindle mount was fixed directly to the nos part of the spindle (as stiff as possible). The back of the spindle mount is fixed to the back 'of the middle part of the housing using a flexible ring to allow for thermal expansion and manufacturing tolerances; To minimize thermal expansion effects 'of the spindle mount itself on radial displacements we choose invar as material' and the mounting plane to machine mount at centre-height of the spindle.
To prevent the machine from heating up by spindle heat losses, ours was provided with cooling channels.

4.3 Design integrated cooling

The friction losses in the bearings and the power loss of the electro motor must be cooled.

preliminary thermal calculations at **IPT** in cooperation with University Aachen (reference 5]) proved the need of helical cooling channels at all bearings and for the. stator of" the electro motor. Since the available space for cooling is limited. an efficient use of the available surface' is needed. To obtain this the cooler channels should be milled at the outside of the workpiece. The minimum distance from the bearing to the cooling channels was **set** to 5 mm for enabling bearing air supply underneath the cooler.
The cooler for the front radial bearing and the front half of the thrust bearing were integrated in the nose, part of the spindle. The inside half of the thrust bearing is cooled by a single channel in the spindle housing. The middle bearing was cooled by a separate cooler either shrink fitted 'or soldered in the housing. The stator cooler was rather" straightforward. Al 1 coolers had separate water outlets for 'coolant flow adjustment.

5. Prototype spindle analysis

5.1, Dynamic rotor/bearing analysis

The optimization tool used a simple FEM model that assumes the bearings to act like pure springs. So we arrived at a natural frequency well above the rotational speed. When we implemented real, bearings in our, rotor/bearing dynamic program RODY we found that the actual situation was far worse, an unstable spindle behaviour was predicted at 100,000 rpm.
On the basis of a one bearing one mass system we optimized the journal bearings for stability" (maximum critical mass) .Small changes in the groove parameters gave stable bearings at the expense of a lower static stiffness and higher power loss. Also the motor connection to the shaft turned out to be' critical needing at least an 11 mm shaft diameter there. Nevertheless we calculated a stable spindle behaviour beyond, the 100,000 rpm even with a two bearing design instead of the original three bearing "design. We choose for the two bearing design because 'that is far easier to manufacture.
For "the thrust bearings we found, that the specified 20 N/µm stiffness' was not enough to have the axial natural frequency above the 100,000 rpm frequency. We needed an "axial, stiffness of 70 N/µm to reach that with a shaft mass of 0.6 kg. We calculated stable bearings at 7 bar by enlarging the thrust "diameter, from 40 mm to 42 mm. .'
Table II gives the calculated properties of the bearings valid for 100,000 rpm rotating speed. The stiffness and damping coefficients (that vary with rotational speed. and excitation frequency) are valid for 20 Hz excitation frequency.
'Around the nominal situation some dimensions were varied to find the tolerances allowed in the manufacturing stage. Especially the bearing gap, heights asked for very narrow tolerances making the manufacturing stage more than a challenge as we expected.
The RODY model (figure 5.1) has 13 nodes and 52 degrees 'f freedom. The cross-stiffnesses (Chv=Cvh) and cross-clampings are not given in the figure but implemented in" the model. It are'

especially the cross-stiffness terms (displacement not in line with load) that determine stability of the system.

bearing	front	back	2*thrust	
outer dimensions	ϕ27*27	$"22'24	ϕ42*ϕ27	.
gap height	5	5	2 * 5	μm
supply pressure	12	12	7"	bara
stiffness Cvv/Chv	96.8/35.2	44.6/19.8	99.0	N/μm
damping Bvv/Bvh	13.28/4.12	12.58/1.80		Ns/mm
power loss	145.3	63.8	151.6	W
friction torque	"13.9 '	6.10'	14.4 ,	N.mm
air consumption	135.6	1 1 3 . 3	183.4	cm^3/s
critical mass	0.46	0'.52 .	infinite	kg

Table II High speed spindle bearing properties

Figure 5.2 gives the calculated deflection over the 'spindle length due to 1 N load at the spindle nose. 'SO the stiffness at the spindle nose is calculated to become about 30 N/μm at the grinding position. Figure 5.3 gives" the mode shape at the lowest natural frequency. calculated to be 1931 Hz (well above 100,000 rpm = 1666 Hz). 'Figure 5.4 gives the frequency dependent compliance at the spindle nose, so excitation at the natural frequency still gives a compliance of 4.10^{-8} m/N or 25 N/μm stiffness .

5.2 Static FE analysis

Both the spindle optimization tool and the RODY tool incorporated a static f-inite'el-ement analysis of the shaft stiffness combined with bearing stiffness... All further FEM calculations were performed with the same MARC 2D FE package at Philips. So for all calculations the same mesh was used.

We calculated the deformation due to the high 'supply pressures (12 bare) acting on the bearing surfaces" and the deformation of the shaft due to centrifugal forces. Summing these deformations (including the deformation due to thermal-effects) gives the bearing gap correction needed for manufacturing to obtain the proposed nominal bearing gaps of 5 μm at running conditions.

5.3 Thermal analysis

The heat calculations for the prototype spindle were performed with a 'heat load of 125 W at the stator part of the motor, 75 W at the rotor part of the motor, 73 W at the back bearing (originally the middle bearing), 165 W at the front bearing and 2*79 W for both sides of the' thrust bearing, so 596 W in total.

We arrived at 98 OC maximum shaft temperature rise (in. the rotor part of the motor) and 26 °C temperature rise at the thrust of the shaft. We found that at "the most critical location the bearing gap clearance will diminish radially 3 pm. Without cooling we expect the total spindle will reach about 700 oC.

6. Prototype manufacturing

6.1 Drawing

Figure 6.1 shows 'the cross section of the final assembly drawing of the prototype high speed spindle equipped "with runout measurement facilities. , The spindle was designed using PRO ENGINEER, a parametric three dimensional design package. During this task several details were established like:

Investigation "into tool fixtures learned that a sphere on cone one was preferred, it was measured to have 40 N/pm stiffness and reproduces its position within ~0.6 pm.. That tool fixture was further evaluated in" reference 6].

Although our starting point was to have the motor positio between two bearings we chose, for a two bearing design with an overhung motor. Dynamic calculations showed that a three bearing design had only a slight advantage in properties at the expense of a more complicated design. So we gained:

Only two bearings need to be aligned during assembling that still remained a matter of extremely high craftsmanship.

The back part of the spindle housing no longer needed 1 µm assembly accuracy.

Balancing of the shaft 'running in its own bearings is needed only once, so only two planes of balancing holes. are needed.

-"The motor fixing is completely changed. From our-supplier we -learned that it was not possible to shrink the motor onto the hardened Stavax shaft at 11 mm diameter because than the magneti losses become very high. So we- changed that into an axial' clamping with an inner shaft diameter of 7.5 mm only, not disturbing the magnetic field.

6.2 Manufacture, assembly and balancing

The manufacturing of the spindle came out to be much more difficult, than we anticipated at the proposal stage. Very ti manufacturing "accuracies were asked for, for instance the th bearing at 7 baro can become unstable at 4 µm gap height and will not give the desired stiffness at 6 µm (at 7 bara supply pressure) . The bearing gaps especially have tolerances on the gap and not on the separate parts (shaft and housing) the gap is made of.

The grinding of the shaft turned 'out to be the most difficult manufacturing challenge especially the. cone with the three notches in front (for positioning the tool fixture) .

We measured the nominal values to be well within specification. From the 5 µm bearing clearances, for all. the bearings we found that in worst case manufacturing 'could"'reduce that nominal clearance 1 µm.

The assembly is performed with pressurized bearings. During

assembly the journal bearings were aligned to a concentricity of 1.6 µm so' 0.8 µm. eccentricity.
The balancing was performed with the spindle mounted upon the math'ine, mount. That assembly was put on its side upon a plate resting on four weak rubbers on a heavy base. The machine mount had two threaded holes in line with the bearing positions to mount acceleration sensors connected to Vibroport balancing u (Schenck) . The rotational speed was measured using a black paint mark at the spindle nose.
The actual balancing was performed at 45,000 rpm and 1 mg accuracy was easily 'achieved. Balancing at higher speeds was tried several times but proved impossible because we experienced that the spindle out of balance was not constant (explained in section 8.1) . ,

7. Prototype high speed spindle tests

During balancing several measurements were performed like bearir flow (as an average measure for bearing gap heights), cooling power, per cooler (heat balance check) and free run down (bearin power loss check) .
Extensive thermal measurements on, the first prototype HSS were made by lPT within a period of 2 weeks at the Philips Researc Lab. in Eindhoven. At different spindle speeds (40.000 to 100.000 rpm) the thermal behaviour of the spindle system was measured. The temperatures at the centre part of the system were detected to be much higher than it could be derived from the calculatic especially close to the. thrust bearing the temperature rises were almost two times as 'high as expected
Unfortunately during investigating erratic frequencies in the ' radial shaft motion (probably noise) , the spindle crashed' at 104.000 rpm. The shaft and the back bearing were damaged at the motor side. That forced us to analyse the cause of the breakdown and to design and manufacture a second prototype spindle

,8." The second prototype

8.1 Prototype breakdown analysis

When the first prototype spindle crashed we already gained three weeks of experimental evidence from which the following conclusions were drawn:
- The heat balance of the spindle did not resemble the calculations. We found as the main cause the extra friction power losses due to free running of the spindle in (supply) air. That accounts for an extra 125 Watt losses compared to 360 Watt bearing friction losses. That extra effective power will also result in higher motor losses. The motor losses were investigated in a dummy experiment at Eindhoven University (reference 7]) .
- The first prototype spindle had a resonance at 95.000 rpm. Experiments and analysis showed that the resonance was due to the housing. Adding an extra mass to the back of the spindle suppressed that problem.
- Balancing was not easily performed. Disassembly of the rotor

from the shaft showed that the rotor could rotate on the shaft. "

In conclusion after adding up the consequence of extra heat loss to manufacturing errors and to assembly errors we could imagine that most of the 5 µm nominal back bearing gap height could be consumed. So we were rather confident that we learned enough to manufacture a better second prototype spindle.

8.2 Design changes

The design of the second prototype (see figure 8.1) resembles the first prototype very much. The main design changes after spindle breakdown were:

-1 Adapting the air bearing gap heights for the higher, heat losses so a new FEM heat run, was performed.
-2 Stiffening the flexure "ring" to shift a housing resonance beyond maximum rotating speed.
-3 Redesign of the motor fixture to improve balancing procedure.
-4 Adapt the cone in front of the shaft for easier manufacture.
-5 Separate 'air 'supply for all bearings to have a check of average bearing clearance (specifically the back bearing) by flow measurements per bearing.

To manufacture a second prototype spindle we used pre-machined parts from our first prototype. We started with finish grinding two shafts from which we chose the best. Although the straightness of the front journal part from one shaft was out of tolerance we preferred to use that one because that error fitted with the calculated gap correction. Grinding the cone for the tool fixture was much easier now because the three notches are set free from the, cone. Machining the nose part and the housing resulted in good parts. All bearing gap heights were realized within the required accuracy.

A problem arose when the outer diameter of the motor rotor was machined. It appeared that our supplier changed their "process so it was, not longer possible to machine the rotor to the optimum 0.1 mm gap. After some delay we got parts from an old batch that could be used.

The assembly went on smoothly and resulted in a better prototype than the one before. We were able to run the spindle at 100,000 rpm without an extra'' mass added. The measured air consumption of the front bearing was higher than calculated but we localised a leakage in the internal air supply circuit, that explains the difference. We found that balancing was improved by the shrink fit of the rotor but further improvement was still needed there.

9. Second prototype spindle measurements

9.1 Grinding experiments

In close cooperation with "a grinding wheel manufacturer (Winter) we choose to" start with a 6. mm tool shaft' with a 3h5 wheel mounting diameter.
Based upon preliminary grinding experiments we' choose for two resilient bond grinding wheel's (K+888 and K730E) and one extremely hard bronze bond wheel' (BZ 387) . Winter not only helped us with the selection but delivered the grinding wheels as free samples.

9.1.1 Grinding experiments (CPE)

At CPE first the aluminum test master for error motion measurements was diamond turned on the spindle running on its "spiral groove motor", so at 5000 rpm. 'The resulting "surface quality was found to be. 3-4 nm Ra. The Rt (Peak to Valley) roughness" was found to be greatly affected by the quality of the aluminium 'material but still 10.9 nm was found. Experience at CPE tells that this was a good indication of the small radial error motion of the spindle. .

CPE also performed the first grinding tests were. The Brite grinding, spindle performed without any difficulties whilst grinding at 100,000 rpm.

Sample number'	Feed rate	Work speed	Wheel ," speed	WYKO TOPO 3D .	Taly-surf ,"	Micro-map 512
	mm/rev	rpm	rpm	Ra/Rt in nm		
1	0.020	300	100,000	6.1 58.6	10.9 9 6 , "	4.7--7.1 48--67
2	"0.008	300	100,000	'3.5 4 5 . 1	8 . 3 "221	4.7--5.3 67--170
3	0.025	100	10'0,000	4 . 1 3.7.2'	101.3 ,92 ,	4.8--4.9 56--85
4.	0.060	100	100,000	24.1 120	2 2 230	23--25 122--169

Table III Surface quality test samples grinded at CP.

Table III shows the evaluation of CPE's grinding results in terms of surface roughness. The WYKO and Talysurf measurements are from CPE and. the Micromap measurement is from Zeiss.
The surface quality produced was in-line with CPE'S previous experience given the specification of the grinding wheel. At such an early stage the flatness of the samples ass very encouraging. The total applied depth of removal was very close to that actually removed.

9.1.2 Grinding experiments (Zeiss\"
Zeiss grinded 9 steel samples. with two different resin bound grinding wheels delivered by the company Winter. Two'g lass" samples were grinded with their own resin bound wheel of 20 mm in diameter. The grinding results are' tabulated in table IV

Sample	Feed rate	Work speed	Wheel speed	Tool	Flat-ness	Rough-ness	Rough-ness
nr '	mm/rev	r p m	rpm	nr	µm	Ra nm	Rt nm
,1	0.09	90	100,100	ϕ7 . 6R	0.3	6 8	3 6 8
2	0.045	180'	100,100.	ϕ7. 6R	0.5	" 2 1	252
3	0.018	180	100,100,	ϕ7. 6R	0 . 9	5 . 3	67
4	0.036	9 0	100,100	ϕ7. 6R	0.4'	8.6	86.4
5	0.09	90	'92,000,	ϕ7. 0A	0.5	' 4 5	226
6,	0.045	180	92,000	ϕ7. 0A	1 . 4	11.5	149.6
7	0.018	180	70,00,0	ϕ7. 0A	1.2	6 0	60.0
8	-0.018	180	92,000	ϕ7. 0A	1.8	..5,.9,	59.4
9	'0.09	3 6	100,100	ϕ7.6R	0.3	6 7	271
G1	0.045	180	53,000	ϕ20.Z	2.2	.2.0	.,45.8
G2	"0.045	180	53,000.	ϕ20.Z	2.2	2.5	74.5

Table IV Results. from grinding tests at Zeiss

Grinding, with the bronze wheel from Winter did not" produce a surface worthwhile to evaluate further. 'The surface roughness achieved with the glass samples were comparable with the best grinded surfaces made at Zeiss until now. Figure 9.1 shows a tangential Micromap track of a glass sample grinded with the 2(mm wheel.

9.1.3 Grinding experiments (Philips),
Philips grinded with 'three types of grinding wheels (K+733E K+888 resin bound wheels and BZ 387 bronze wheel) on BK7 glass and stavax (hardened steel). Philips experienced a large improvement in grinding results:
- The' grinding marks are very regular because of the. constant speed of the spindle.
-, The high stiffness of this spindle changed the form error from a compliance dominated error (resulting in a convex shape instead of flat) into a wear dominated error (concave shape) . Also sparking out did not occur.
- 'A very good surface quality is achieved, grinding stavax with K+888 wheel produced "'lapped" surface quality.

These experiments showed that the spindle is no longer the weakest point in their grinding process. A theory based on a wear dominated grinding process, came up with a model to predict from errors during grinding that could be used for 'feed forward compensation.

9.1.3 Analysis" of grinding results,
The samples grinded by CPE (4 steel samples) and Zeiss (9 steel, samples and 2 glass samples) are analyzed for surface roughness. The roughness in feed direction is found to be mainly dependent on feed rate and radius of the. grinding wheel. The measured values agree with calculated theoretical values with only" 10% deviation.
The surface roughnesses in 'the valley of a feed' mark shows a periodical pattern with a wavelength corresponding exactly to the feed for one revolution of the grinding wheel (figure 9.2) . The peak to valley of "this roughness is a good indication of the error motion of the spindle plus roundness of the grinding wheel. At low feed rate a roughness 5 nm Ra was measured. The glass samples grinded at Zeiss with a 20 mm diameter wheel even a'thieved 2 nm Ra roughness;
The analysis of the roughness measurements "for the samples grinded by Zeiss. and CPE shows the high potentials of our spindle,.

9..2 Thermal' measurements (IPT)
The thermal measurements were focused on. (thermal) displacements. During speeding up the axial, z-deviation"of about', 15 µm is dominant see figure 9.3. The deviation in the vertical -y-direction stays in the range "of 3.5 µm. As the displacement of the" mount support is part of that vertical shift, 'a reduction 'should, be possible by cooling that mount. The horizontal x-displacement stays in the sub micron range. The spindle reaches. 'rapidly a thermally stable situation after each speed change. At constant speed the thermal displacement in axial z-direction amounted '0.5 µm/deg and in horizontal x-direction far less. The axial z-displacement directly depends on cooling water temperature (figure 9.4) with very short response time (seconds) . The vertical y-direction shows a constant growth rate of 0.1 µm/min, mainly caused by thermal drift of the mount. With an accurate cooling water temperature control (to 0.02' deg C needed) plus a cooling of the mount the thermal behaviour of this spindle will be within the 10 nm specification.

9.3 Dynamics stiffness measurements" (IPT) '
The dynamic' spindle stiffness **was** measured by machining an aluminium master on the HS-spindle at different spindle speeds. During the cutting. process, the tool was excited with a white noise signal and a dynamic force was implied to the spindle. Simultaneously, the deviation of the master was measured. The' analysis" of the force and deviation signals was executed using a Fourier-analyzer.
The spindle stiffness could be clearly determined as a "function

of. the spindle speed between 0 and 65000 rpm (figure 9.5). higher spindle speeds, the increasing dynamic 'forces prevent further measurements with the chosen method. The stiffn changed from 5,6 N/µm at zero-speed to 15,6 N/µm at 65000 rpm. From the obtained results it can be deduced that the aspired stiffness of 30 N/pm at. 100000 rpm will be achieved. The measurement results of the low frequency stiffness match t calculations done by Philips. :

9".4 Error motion' measurements (CPE)
CPE developed its own software to' measure the spindle error motions up to' maximum, speed of 100,000 rpm. That concerns 'bo radial and axial, synchronous and asynchronous, error motions with nm resolution. The software was tested on the error motion of a standard running spindle. '
The ADE measurement probes were calibrated against a Hewlett Packard Laser System. The system is first tested with lower speed' spindles and proved to operate to expectations.

The final phase of error motion measurements was performed by CPE at Philips location. The master piece was first turned round. Measurement of the surface roughness of that in situ 'diamond turned master on a Wyko gave 4.9 nm Ra or 30.5 nm peak to vall Out of four measuring configurations the best one was, chosen that gave minimal noise (typically ,2.2 nm synchronous noise and 5.6 nm asynchronous noise).
The measurements were performed under four conditions. First when the spindle was free running at its own 5000 rpm driven by the air supply acting on the 'spiral grooves in the bearings. Next a series of three speeds' 50,000 75,000 and 100,000 rpm, driven by the two pole asynchronous motor'.

spindle speed	error motion measurement results			
	measured error		error after correction	
	synchronous	asynchronous,	synchronous	asynchronous
5,000	8.56	, 10.56	23.58	, 10.45
50,,000	41.59'	39,.73	'2725.55	3939.73
75,000	90.81	68.57	74.85	68.6857 ,
100,000	, 52,0,8,	" 39.18	73.33	" 38.04 ' ,.

Table V Error motion measurement results

The measurements with the free running spindle gave excellent "figures close to the noise of the measurement system. '
We experienced the worst behaviour at 75,000 rpm and at higher speeds the error motion decreased but remains above our specification (synchronous error 50 nm and asynchronous 20 nm) .

We found a two lobed shape of the errors (probably the two poles of the motor drive) that rotates several degrees per revolution (probably the slip between magnetic field and rotor speed) as can be seen in figure 9.6. So the amount of asynchronous error very much depends upon the number of revolutions "considered. In other words all the errors become asynchronous "error with long observation time.
The master was carefully calibrated afterwards on a sperate set-up. That calibration gave an "error magnitude of 26 nm. The shape of that error was mainly elliptical. Next step was to subtract 'numerically that master error from the measured data 'to 'obtain a corrected error motion of the spindle. That resulted in the. corrected data.
Finally an effort was made to eliminate the phase shift per revolution. from the measured data to get an indication what error will result with a synchronous motor drive at 100,000 rpm. That numerical "calculation' came up with an synchronous error of 45.07 nm (within the spec of 50 nm).

The error motion measurements learned that the shape of the profile rotates a few degrees per revolution. This can b explained by the theory from R. Belmans (reference 8] , 9] ar 10]). **It** could be caused by" the homopolar magnetic field that results in motor forces' that rotates with twice the slip-frequency' at a dynamic eccentricity. In future designs one needs electro magnetic expertise to suppress this effect.

10. Final spindle redesign

10.1 Design changes

A part of this task was already performed .when we designed the, second prototype spindle. That spindle was used extensively and gave good confidence in its potentials. It was evident however that this prototype spindle was not suited for production grinding.
The manufacturing costs reduction was discussed extensively. The design with its tight tolerances resulted into' very high manufacturing "costs. The spiral groove bearings can not be reduced in accuracy or complexity. They are one of the main surfaces for proper function of the spindle. We also experienced that sensor holder and machine mount were adapted by each partner so we decided that such parts. do not longer belong to the spindle itself. The thin shaft diameter at the motor location made the grinding of the shaft difficult.
It was a **Pleasure to learn** that Hembrug put, much effort in analysing the drawings of the Brite spindle. We did benefit a lot from this work hidden in the following consolidated cost reduction design proposals:

-1 The motor fixture will be performed by 'a long thin bolt . pressing the rotor against the back of the shaft.
-2 Integration of motor cooler, and stator cooler was pursued as major part in the spindle redesign.
-3 We learned that a standard spindle has only a mounting face

and threaded holes at the back (the user can design his own specific flexible support) . So the invar spindle mount plus expansion ring were no longer integral part of the, spindle' for more flexibility.

-4 All supply and return channels should preferably be axially" connected at the back of 'the spindle.

-5 We preferred to use 6 in stead of 8 holes in the nose plane leaving more space for the supply and return channels. At the back the 4 locations for flexible mounting could be' minimized to three.

-6 We choose a simple tool fixture comprising only a bolt that is centred in the shaft. The small dimension of the bolt will not cause unbalance problems larger than from the grinding wheel itself.

In conclusion we felt that we found a good combination of manufacturing costs reduction and improved spindle design. The consolidated changes will also result in a spindle that is better suited' for production use.

10.2 Analysis of the redesigned spindle

For. the redesigned spindle new calculations were performed to arrive at the gap corrections needed to manufacture the housing bores from the measured shaft dimensions. The calculated gap corrections for the redesigned spindle are given in figure 10.1. The gap corrections, result from pressure deformations (0.5 µm) plus deformation due to centrifugal forces '(2.5-2 µm) plus thermal deformations (2.5-2 µm).The total deformation is approximated by straight lines (constant over the spiral grooved part 'of the bearing' surface) .

A cross "section of the redesigned spindle is given in figure 10.2.

Figure 10.3 shows, the calculated temperatures plus the mesh used for, calculation (3419 elements with 3795 nodes) ., The windings of the motor become the highest' temperature rise of 120 degrees C, and we find a 'considerable temperature drop across the air bearing gaps. Input for the heat calculation were 75 W for motor rotor, 200 W for motor 'stator. and 145 W for the front bearing, 64 W for the back bearing, 76.6 W for" each side, of the thrust bearing' and 125.8 W distributed losses around the no bearing parts of the shaft.,

10-.3 Manufacturing

The manufacturing. of-four optimized spindles was performed at the research workshop of Philips. The rotors from the motor were shrink fitted "to the shaft and that assembly is ground to final dimensions" with better roundness and squareness as for the prototype spindles. Figure 10.4 shows some manufactured parts, nose, housing and cooler bushing.

The critical phase of the 'assembly of the Philips spindle was attended by the specialists from CPE, IPT and Zeiss.', An assembly, manual was written. Figure 10.6 shows the assembled redesigned spindle.

The balancing was performed in two steps only. First balancing

was performed at **40,000** rpm where, 28.5/47.6 mg was measured to be removed in both measurement planes. (almost 'in line with the radial bearings) . That was a large amount because the weight of a single balancing screw is about 80 reg.. Thereafter we balanced again at 75,000 rpm and had to remove only a few mg's. In conclusion we feel that the redesigned motor clamping made the balancing much more. easier than with the prototype spindle. '. An assembled spindle with user dependent accessories (piping, spindle mount and machine mount) can be seen in figure 10.5. In the machine mount are two cooling channels that provide' thermal isolation between spindle and machine. .

11. Optimized design tests

11.1 Measure thermal behaviour

At IPT a set of measurements on thermal stability of the spind were performed similar to the prototype spindle measurements. The meas-urements taken at 40,000 rpm show a similar thermal behaviour of the IPT spindle. in 'comparison to the prototype spindle. The displacements in x- and y-direction stay below 0.3 µm during the-whole" period. 'The deviation in z-direction 'is mainly influenced by the water cooling system. The waves with an amplitude of about 0.4 µm in the z-deviation curve follow directly the temperature of the cooling water **(0.7** K wave amplitude).

To prove the application of the cooling system for the spindle mount, the measurements at a spindle speed of 70,000 rpm" were taken. The prototype spindle was running at 100,00,0 rpm without this cooling system. From the obtained curves it can be seen that the mount cooling, reduces the thermal drift in (vertical) y-direction. On, the other side, the influence of the water cooling cycle can be found in a wavy structure of the same displacement curve,.

11.2 Grinding'tests

The second prototype' spindle was tested at **Zeiss** with a . production, machine for precision grinding under workshop conditions. The achieved results with test pieces made of steel are very exciting, because we never expected to get good ground surface of steel with diamond grinding wheels. The ground surfaces of glass were the best Zeiss ever made. All of these are good indications for the good behaviors (error motion and stiffness) of the high speed spindle. We expect that the redesigned spindle should make at, least the same or. better results.

11.3 Measure error motions

At IPT run-out measurements of the HS-spindle were made with a master-cylinder which was machined on the H'S-spindle. Due to this the synchronous error of the spindle run-out can not be detected but balancing is much easier. As the noise level (asynchronous error) resulted to about 150 nm the set-up has to be optimized. More measurements will be performed after, the project ends.

11.4 Measure dynamic behaviour

IPT measured the zero speed stiffness to be 10 N/pm so higher than the 7 N/pm of the prototype spindle. The compliance measured did not reach the static value for frequencies up to 1900 Hz. Over the whole range no 'sharp peaks were found. The peak at about 1200 Hz.was found to originate from the spindle mount. A well damped resonance frequency at about 150"0 Hz was determined ' to be the first bending mode of the shaft plus rotor assembly.

12. Conclusions

The new design of the motor fixture made balancing much easier. The thermal properties of the spindle are good but can still be improved by a more accurate temperature control of the cooling fluid. The dynamic behaviour (stiffness) of the spindle is'better than specified. The runout of the spindle is that good that electro magnetic noise prevents us for stating an accurate value. The only drawback is the seizure of the spindle at Philips, so limiting the maximum speed to 90,000,rpm is advised. The grinding results of the prototype spindle were already excellent. The redesigned spindle is expected to produce at least similar results with a far more user friendly design.
The properties of-our spindle are' summarised below.

Maximum rotating speed		90,000rpm
Radial stiffness at cutting edge		> 30 N/µm
Axial stiffness at cutting edge (calculated)		60 N/µm
Error motion asynchr. + synchr.		120 nm
Thermal drift at 70,000 rpm with 0.7 K coolant temperature variations '.	axial	0.8 µm
	vertical.	0.4 µm
	horizontal.	0.3 µm
Thermal time constant '		≈ 10 sec
Grinding performance		very good

It is evident that many persons collaborated' to achieve this result. Several changes in personnel occurred during the project but the least I can do is to acknowledge the project leaders that made it to the project end.

Cranfield Precision Cranfield : Keith' Carlisle
Fraunhofer IPT Aachen : Hans-Bernd Schroder
Carl Zeiss Oberkochen : Dr Yaolong Chen
Philips. Research Eindhoven : Peter Holster

References :

1] Franse J.; Aspects of Precision Grinding , Thesis from Technical University of Eindhoven 5 July 1991

2] Bartholomeus R.P.M.; Rotor-lagerdynamica binnen PC-matlab (Rotor-Bearing dynamics in PCmatlab) WFW report 92.019 TU Eindhoven, The Netherlands

3] Bartholomeus R.P.M..; Ontwikkelen van lagermodellen in' het pakket RODY-III (Development of bearing models within thew RODY III package) WFW-rapport 93.033 TU Eindhoven The Netherlands

4] Geerts N.; Linear Dynamic Analysis "of Rotor systems with Gas Bearings, Master's Thesis WFW report 95.090; WFW (Department of Fundamental" Mechanics) Faculty of Mechanical Engineering Eindhoven University of Technology.

5] Frenz M. ; Rechentechnische Analyse des thermischen Verhaltens einer Hochfrequenzschleifspindel fur die Ultrapräzisionstechnik sowie Dimensionierung der Z u thermischen Stabilisierung erforderlichen Kühlung (Thermal Analysis of a high speed grinding spindle for ultra precision machining including the dimensioning of the coolers for thermal stabilization) Studienarbeit March 1993 RWTH Aachen

6] Hoog J.R.de; Kwantificering van een slijpsteen spanpunt (Quantification of a tool fixture) . Stage report Technical University Twente **1995.**

7] Smulders H.W.M.; Stage report EMV **94-05:** Verliezen in kleine, sneldraaiend kortsluit-anker motoren (Losses in small high speed induction motors) ,TU Eindhoven

8] Belmans R.,; Radiale trillingen van driefasige, tweepolige inductiemachines met kooianker. (Radial- vibrations of three phase, two poles induction 'machines with cage rotor) at the Katholic University of Leuven (UDC.621.313.3) thesis dated' December 1984

9] Belmans R., Geyser W., Jordan H., Vandenput A.; Unbalanced magnetic pull in three phase two pole induction motors with eccentric , rotor. Proc. International Conference on Electric Machines; Design and Applications London, 13-15 July 1982, IEE Conference Publication, Nr 213, p65-69.

10] Belmans R, Geysen W., Jordan H., Vandenput A.; Unbalanced magnetic pull and homopolar flux in three phase induction motors with electric rotors. Proc. ICEM, Budapest, 5-9 September 1982, p916-921.

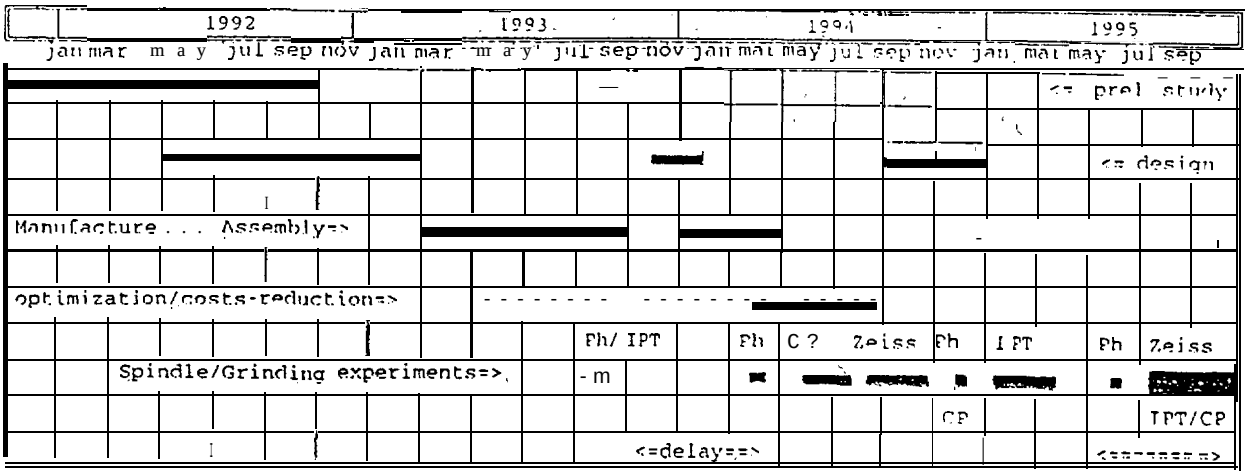

Figure 2.1 Time chart of, the project

Speed		
Maximum rotating speed	100.00.0	rpm
Accuracy-speed control;	1	%
Stiffness, measured at cutting edge position		
Radial stiffness (at rotating speed)	20	N / p m
Axial stiffness (at rotating speed)	20	N/pm
Tool specification		
Small grinding wheels (with shaft mounting)'		
Wheel diameter	6-20	mm
Mounting reproducibility"	1	µm
Mounting stiffness	20	N/µm
Large "grinding 'wheels (with internal mounting'),		
Wheel diameter	20-.50	mm
Load		
Maximum load at cutting edge position	1	N
Resolution measuring facility for axial and' radial load	.01	N
Balancing		
Resolution dynamic balancing	.05	N
Error motions		
Radial 'synchronous error motion	50	nm
Radial asynchronous error motion , ,	20	nm
Axial. total error "motion	30	nm
Resolution radial (two planes) and axial position measurement (during valuation)	1	nm
Thermal drift in radial and axial direction (to be measured after 15 minutes) ' ,	10	rim

Figure 3.1 High Speed Spindle specifications

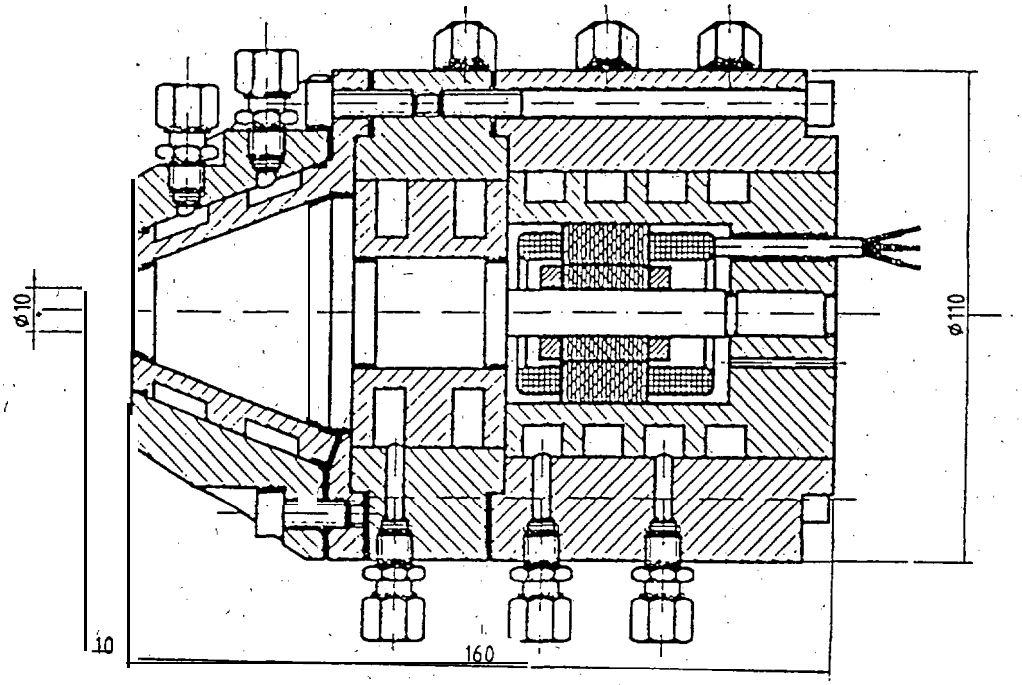

Figure 3.2' Preliminary design chosen for further evaluation

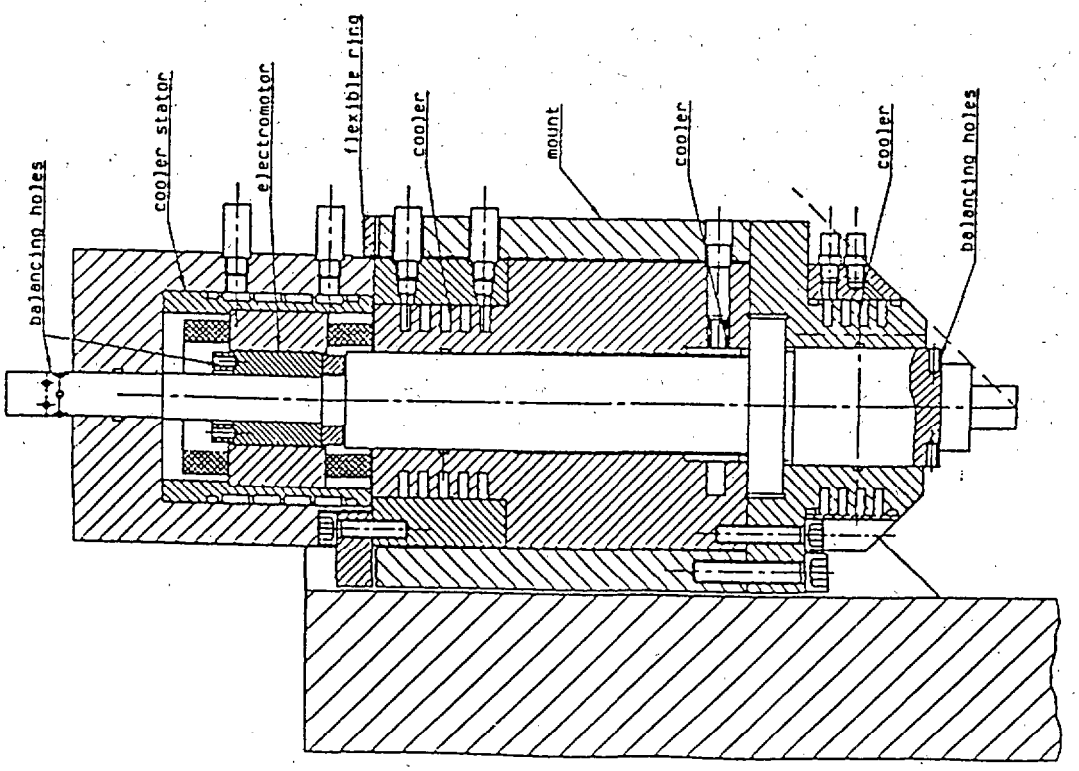

Figure 4.1 Three bearing design

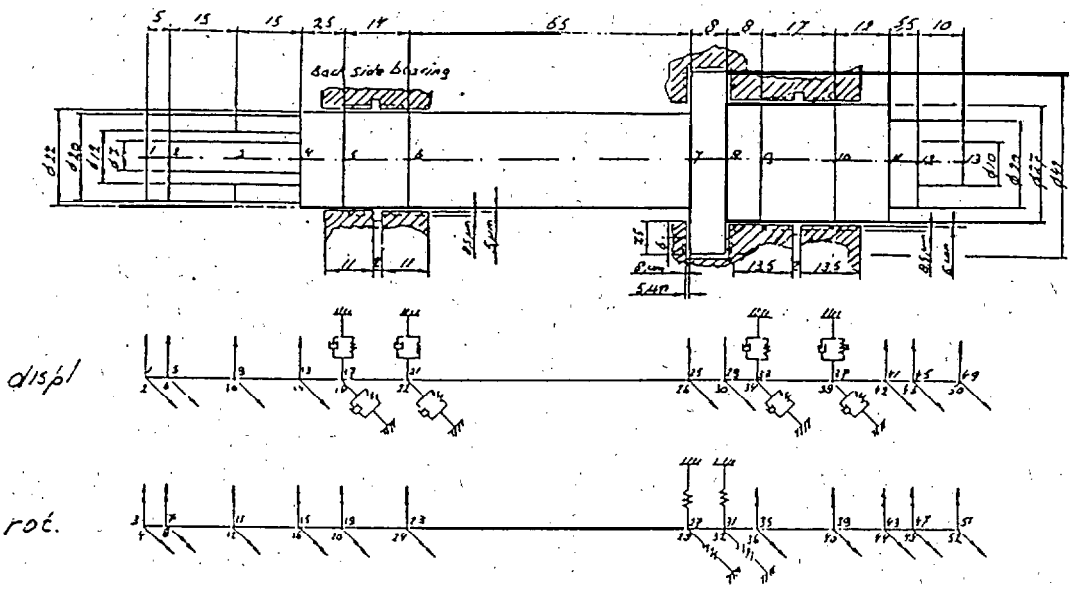

" Figure 5.1 RODY model for rotor bearing dynamics

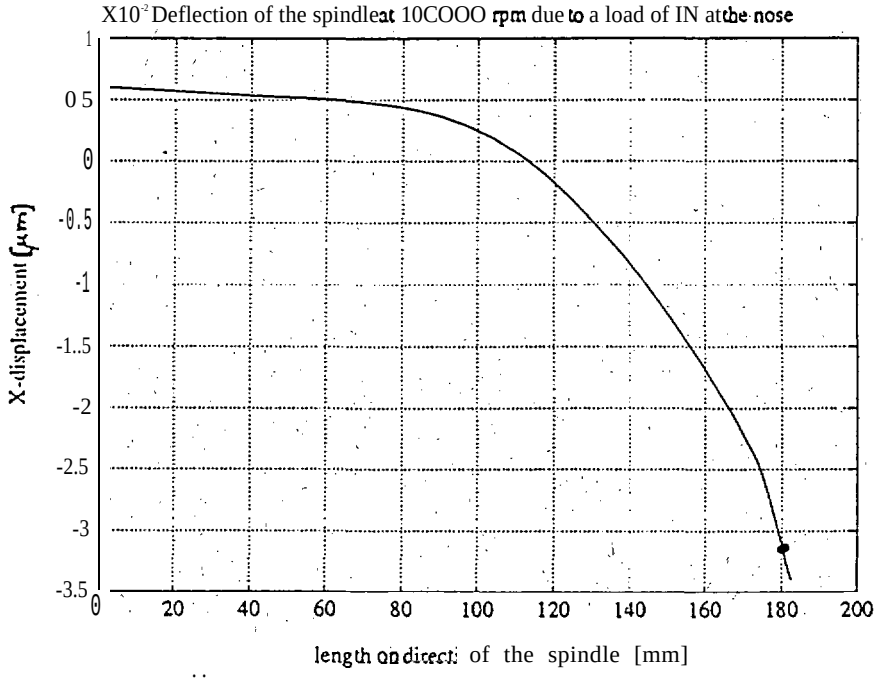

Figure 5.2 Calculated spindle deflection over its length

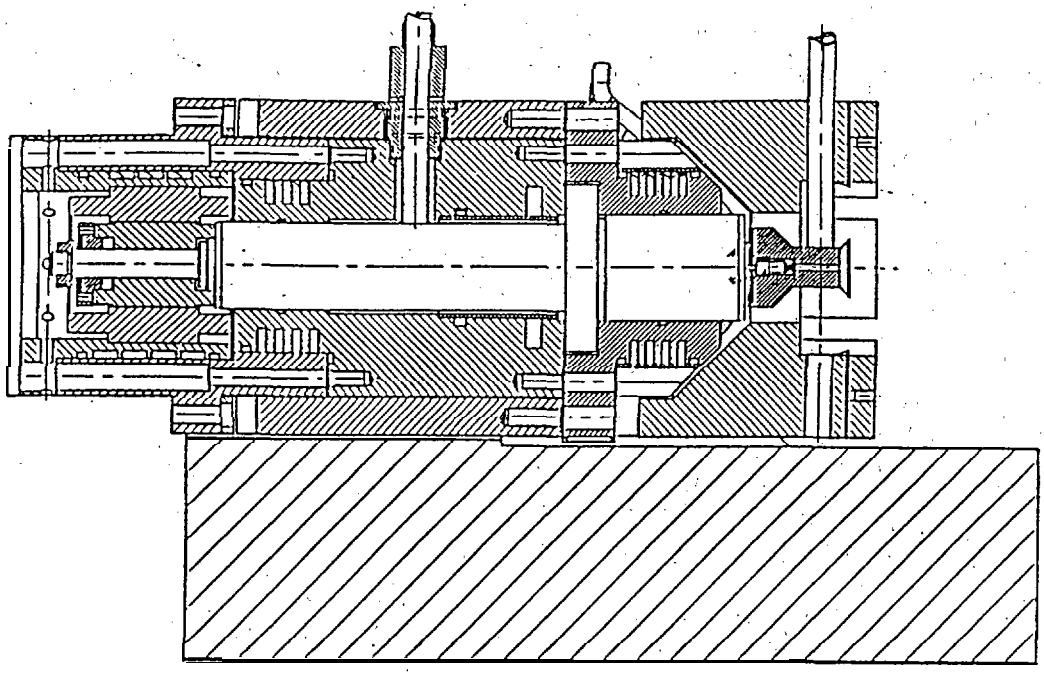

"Figure 6.1, First, prototype design equipped for runout measurement and machine mount

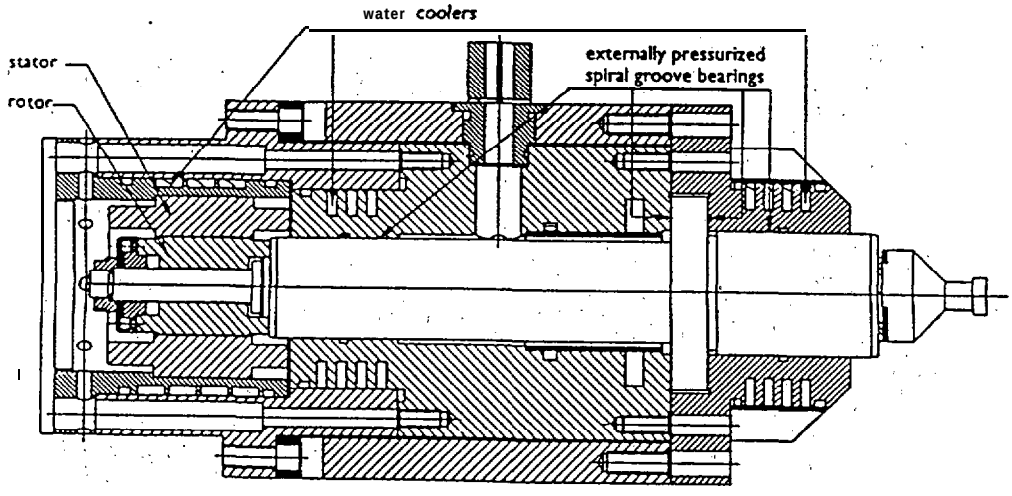

Figure 8..1 Second prototype design

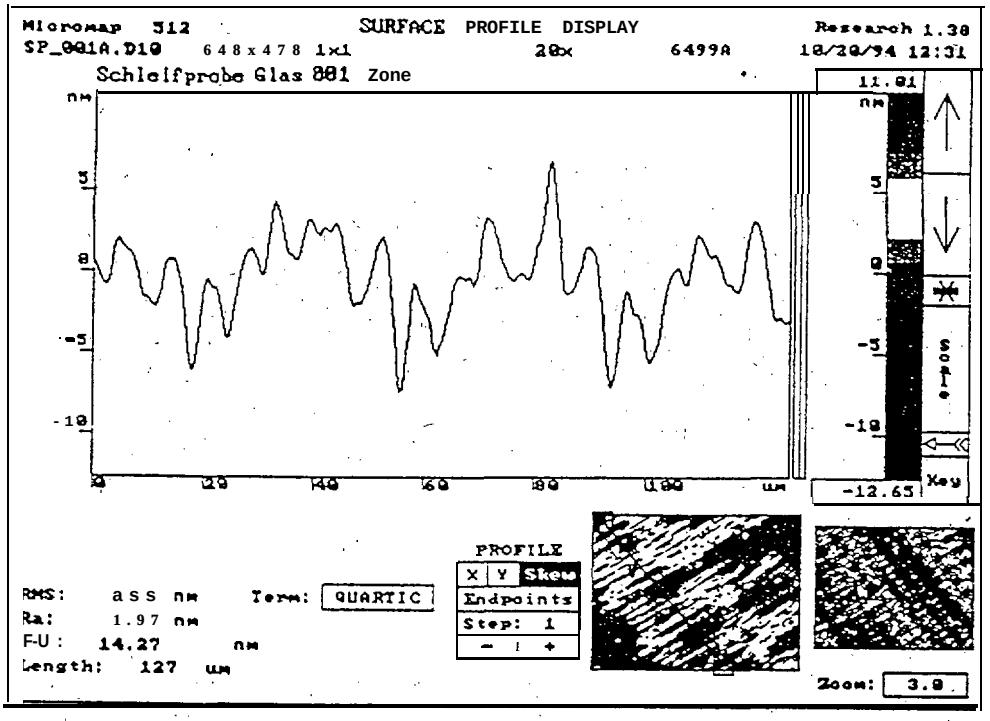

Figure 9.1 Roughness in the valley of a feedmark from Zeiss sample G2

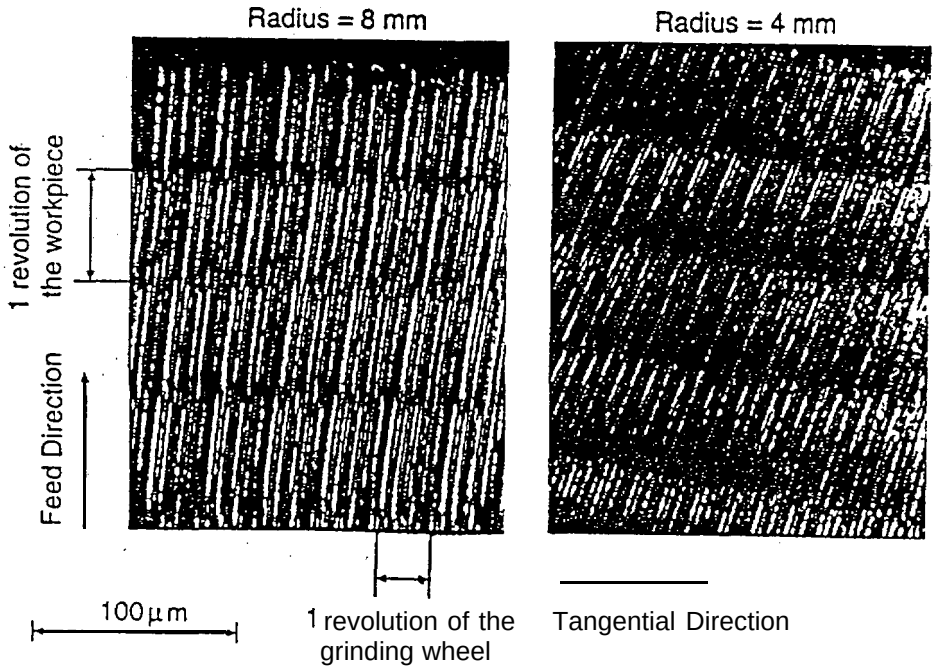

Figure 9.2 Grinding marks from **CPE** sample 4

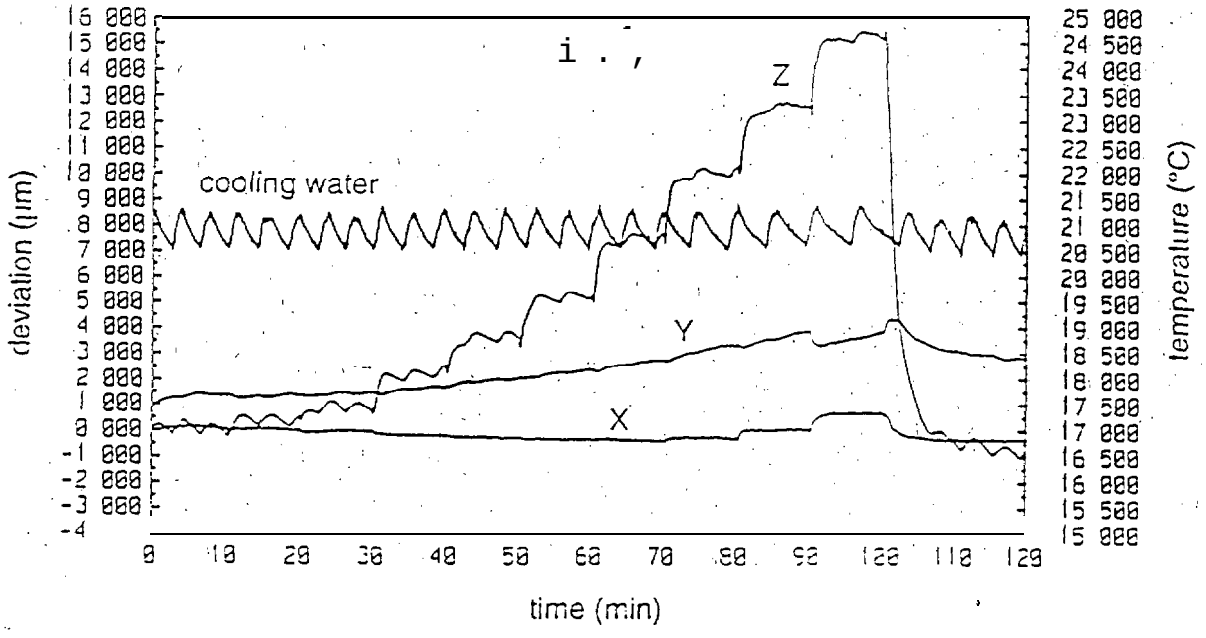

Figure 9.3 ..Thermal deviation at speed **Up**

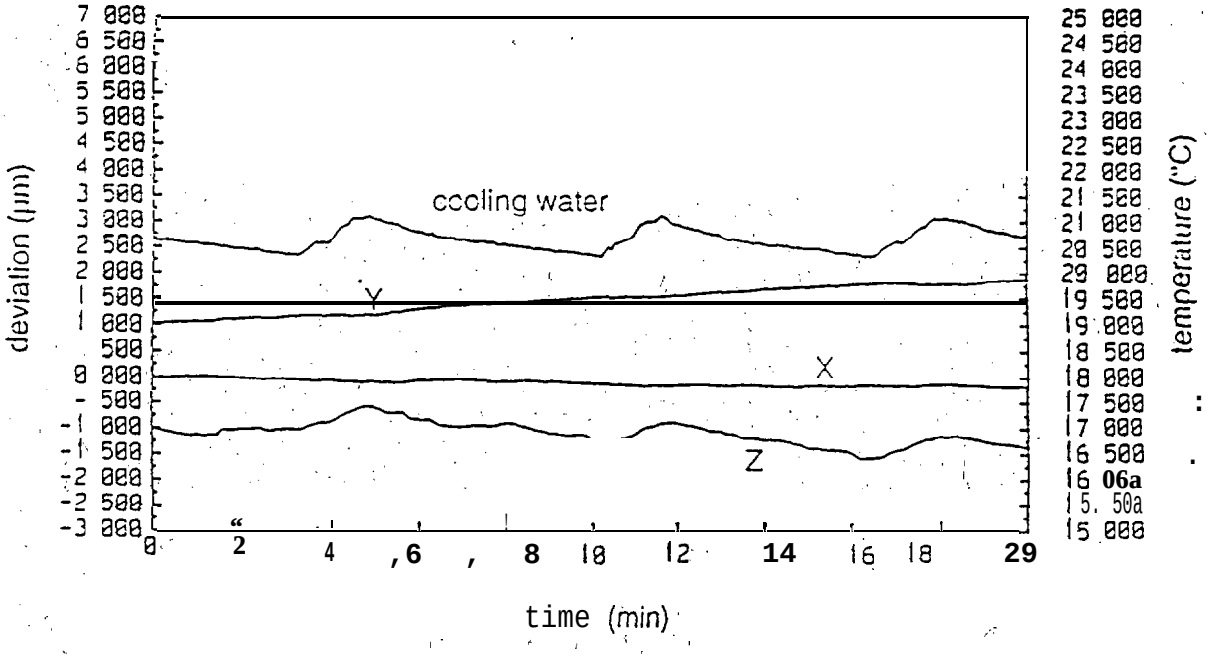

Figure 9,4 Thermal deviation at constant speed

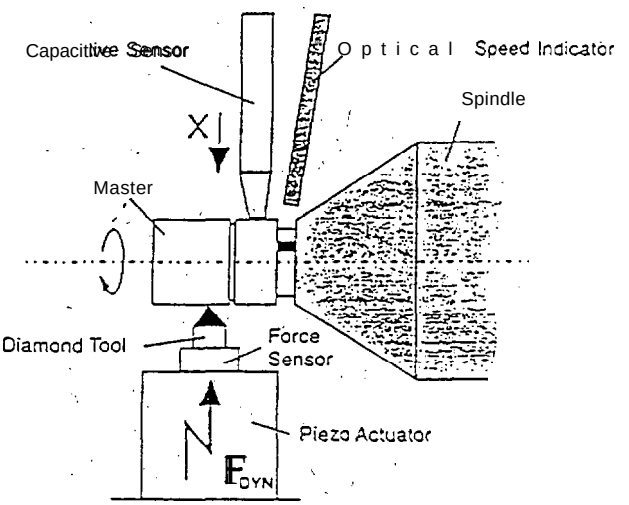

Figure 9.5 Stiffness measurement set-up

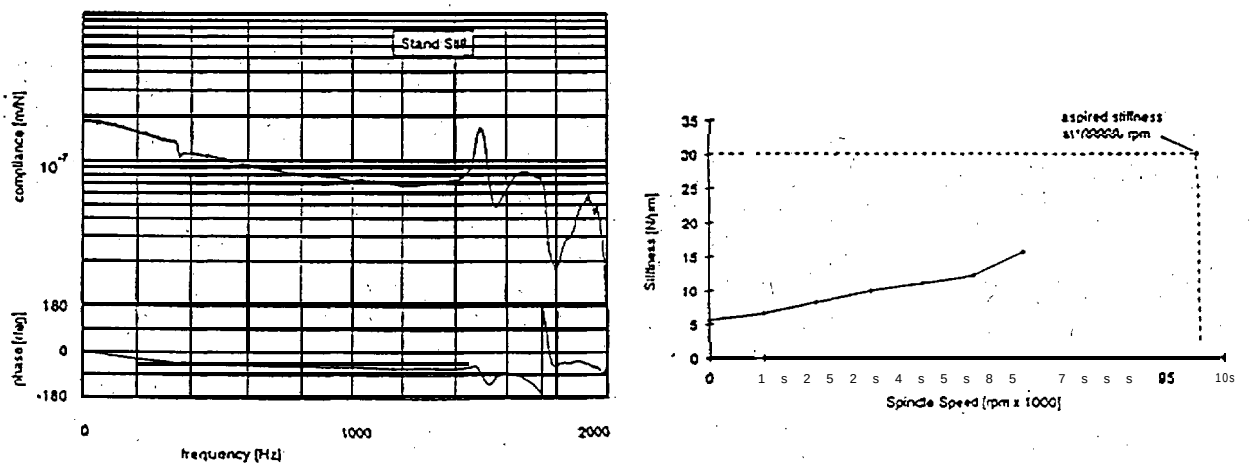

Figure 9.6 Stiffness measurements at cutting position
Left: Dynamic compliance at stand still
Right : Stiffness at various speeds

Project: UP20871

Customer: brite

Serial Number: 002

Location: Philips

Date: 13-CM-94

By: Jack & Paul

Measurement: Radial - X Direction

Spindle Speed 9.595e+004 rpm

Asynchronous Error: 38.04 nm

Synchronous Error: 73.33 nm

Number of Cycles: 5

Points per revolution: 250

Filter: 60 UPR

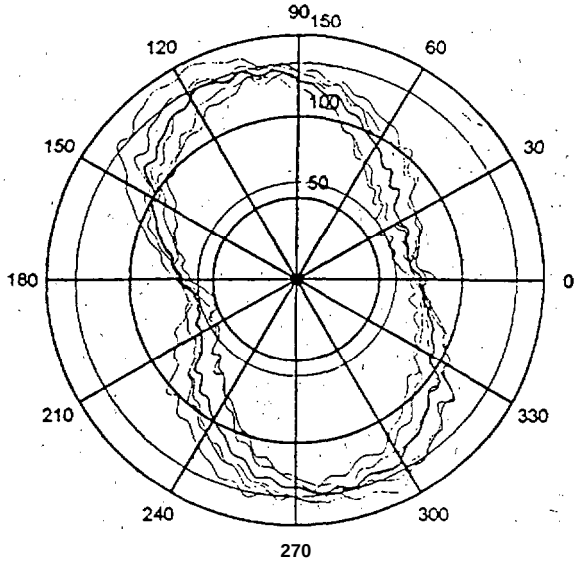

Figure 9.,7 Typical error motion profile at 96,000 rpm

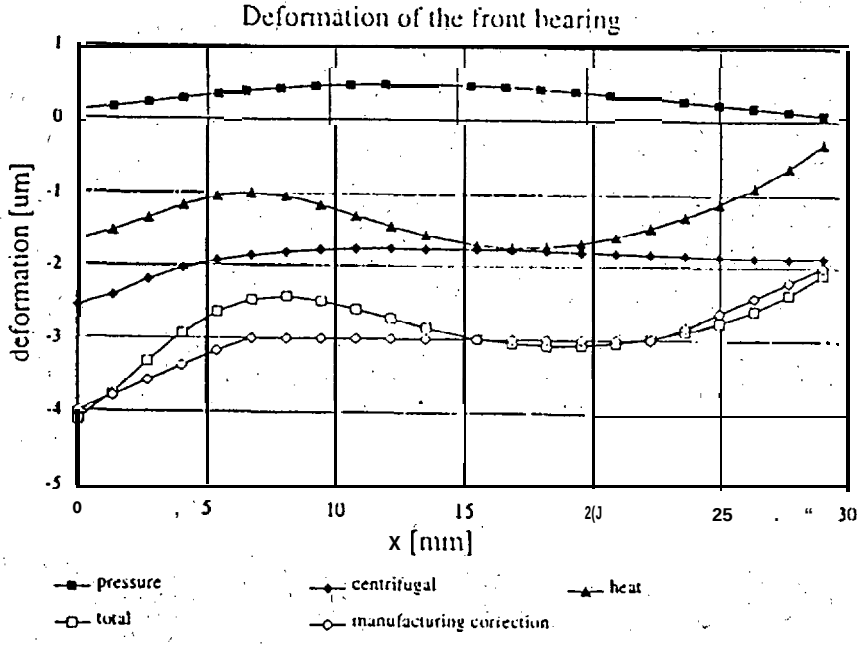

Figure 10.1 Gap corrections

intentionally left blank

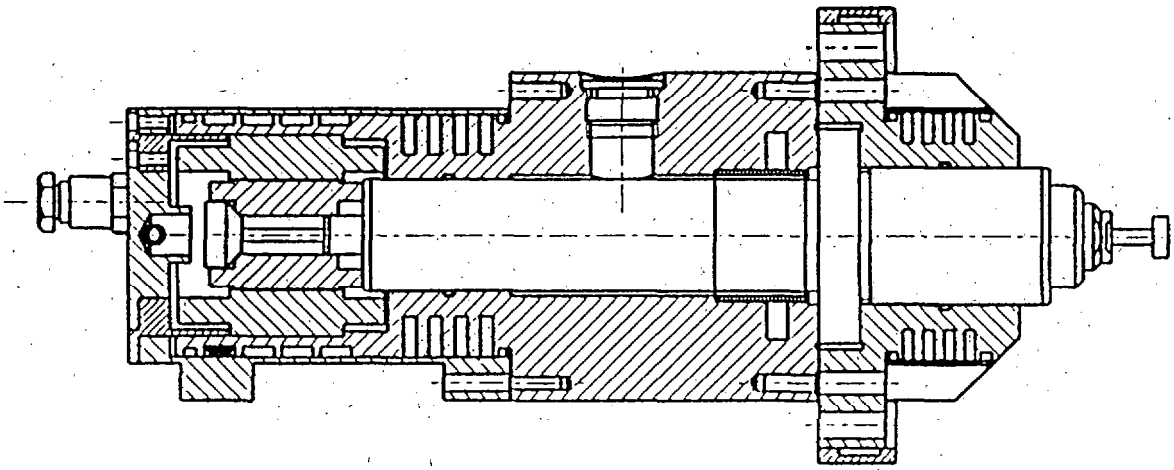

Figure' 10.2 Redesigned spindle

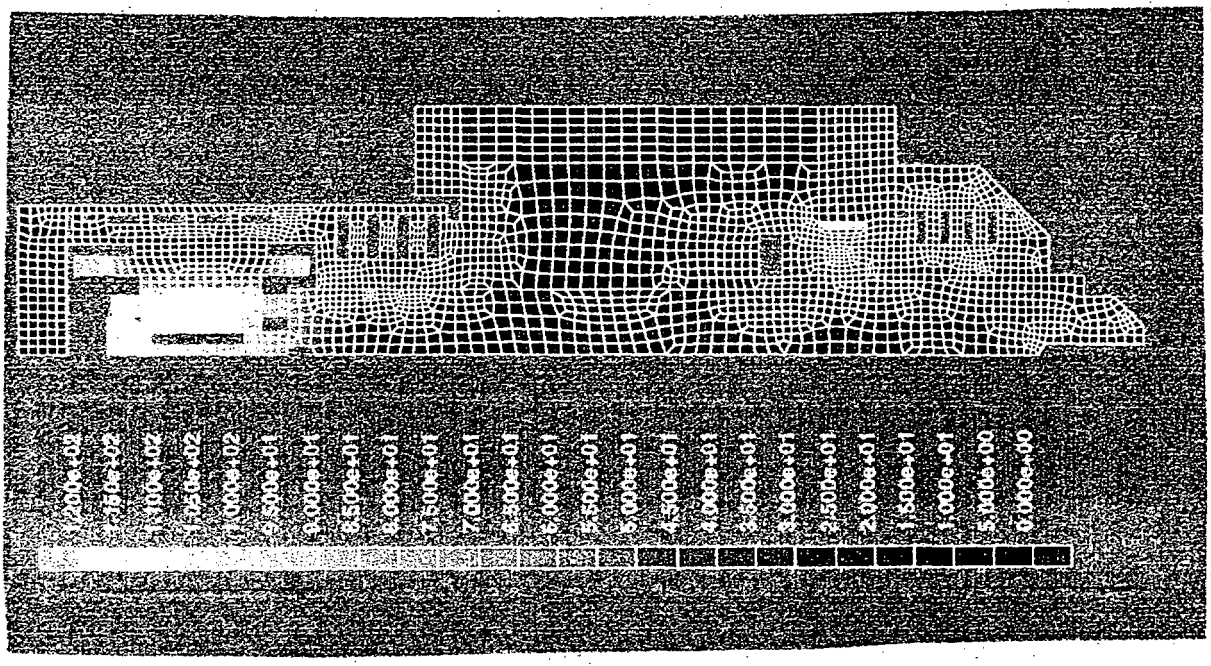

Figure 10.3 Calculated temperature distribution

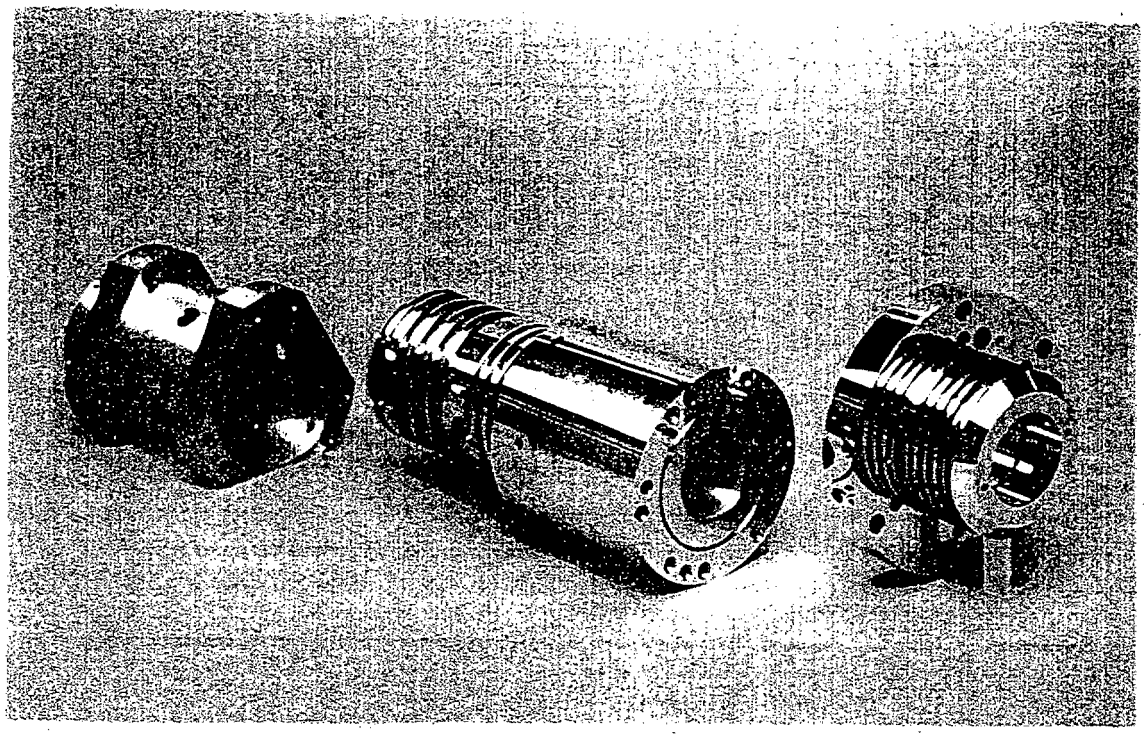

Figure 10.4 Spindle" nose, spindle housing and cooler bushing

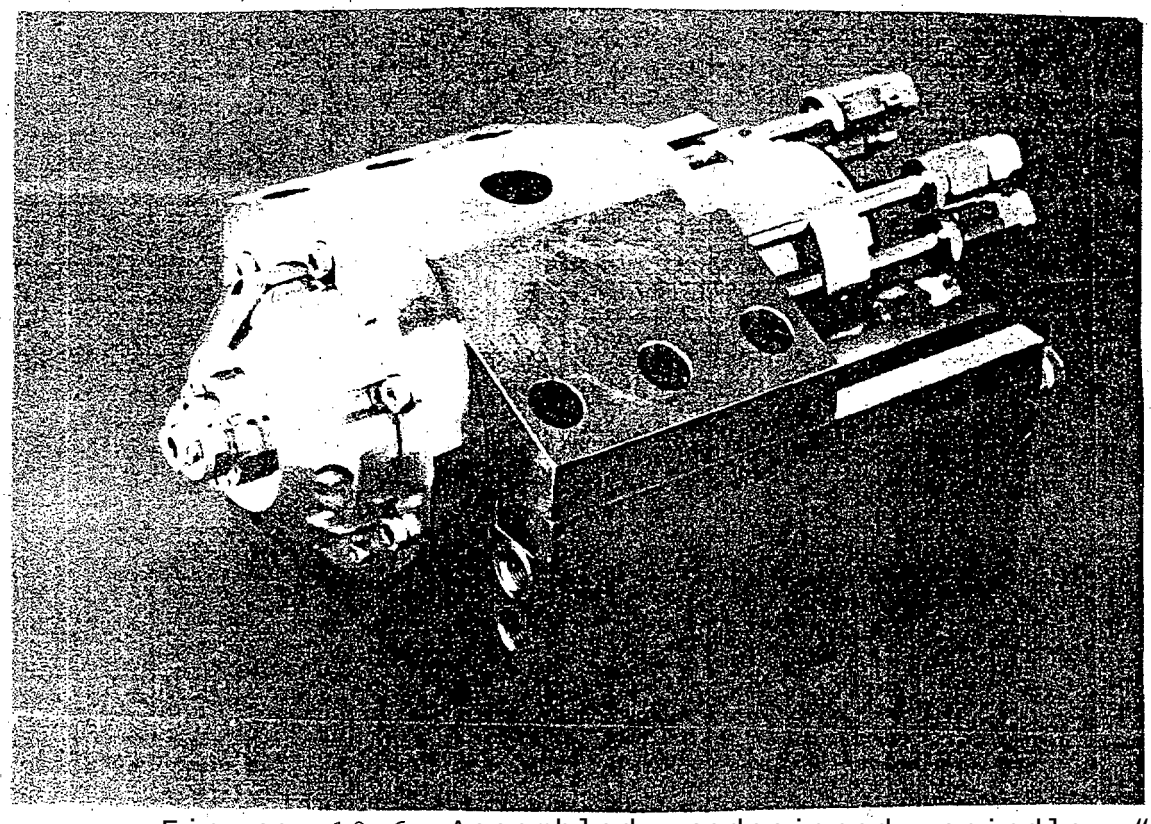

Figure 10.6 Assembled redesigned spindle "